Chapter

Natural Polysaccharides in Breast Cancer: Fucoidan's Role in Enhancing Cisplatin Cytotoxicity and Reducing Chemotherapy Resistance

Reza Taghipour, Hadi Hassannia, Hesamoddin Arabnozari, Seyed Ehsan Enderami and Emran Habibi

Abstract

Cancer is one of the leading causes of death worldwide. Recent advancements in chemotherapy, particularly using natural drug-based strategies, have shown promise. This study evaluated the antitumor and anti-inflammatory effects of a combination of the brown alga *Sargassum ilicifolium* with cisplatin *in vitro*. After collecting and identifying the algae, fucoidan and alginate were extracted. The antioxidant activity was assessed using DPPH and Ferric Reducing Ability of Plasma (FRAP) assays. The cytotoxic effects on the MDA-MB-231 breast cancer cell line were evaluated in both 2D and 3D cultures using the XTT assay. Fucoidan and alginate yielded 7203 and 441 mg per 100 grams of dried algae, respectively. Total polysaccharide content in the fraction was estimated to be 89.39 mg/g dried algae weight. Fucoidan-rich extract exhibited higher antioxidant properties compared to alginate-rich extract. Also, the combination treatment significantly enhanced cytotoxicity, with the IC_{50} of fucoidan-rich extract reduced from 177.9 ± 8.7 to 79.3 ± 4.6 μg/ml in 2D culture when combined with cisplatin. In 3D culture, the IC_{50} decreased from over 800 ± 78.5 to 364.5 ± 41.7 μg/ml. Additionally, the fucoidan-rich extract significantly decreased IL-1β and IL-6 cytokine secretion in macrophages. These findings suggest combining cisplatin with fucoidan-rich extract enhances antitumor efficacy and may reduce chemotherapy side effects.

Keywords: alginate, breast cancer, cisplatin, fucoidan, MDA-MB-231

1. Introduction

Cancer remains one of the most critical global health challenges, with over 10 million new cases diagnosed annually. Cancer development is primarily driven by

mutations in oncogenes that lead to a dominant gain of function, along with the dysfunction of tumor suppressor genes [1, 2]. Among women, breast cancer is the most common malignancy worldwide and is the leading cause of death from cancer. The incidence of breast cancer continues to increase globally, with more than one million new cases each year, accounting for approximately 25% of all cancers in women [3, 4].

Triple-negative breast cancer (TNBC) includes various diseases that differ in histologic, genomic, and immunologic profiles but share a lack of estrogen, progesterone, and HER2 receptors. TNBCs generally have a 5-year survival rate of 8–16% lower than hormone receptor-positive cancers and exhibit aggressive clinical behavior. They are more common in younger women and those of African or Hispanic descent, and they are the most frequent invasive breast cancer type in patients with BRCA1 germline mutations [5, 6]. MDA-MB-231 cells serve as a critical model for the mesenchymal subtype of triple-negative breast cancer (MES-TNBC). Due to its representative features, this cell line is widely used to study the characteristics and behaviors typical of MES-TNBC [7].

Chemotherapy often targets DNA, causing mutations or genome instability, a hallmark of cancer and aging. Various chemotherapeutic drugs are genotoxic, disrupting DNA metabolism through different mechanisms, each with unique biodistribution and kinetics [8]. Chemotherapeutic drugs are administered either before surgery (neoadjuvant therapy) or after surgery (adjuvant treatment) to selectively inhibit cancer cell proliferation and induce apoptosis. However, patients often experience moderate to severe side effects and may develop acquired drug resistance due to prolonged treatment [9]. Cisplatin, a platinum-based drug, works by binding to DNA and forming platinum-DNA adducts, which cause DNA damage, lead to G1/S phase arrest, and trigger apoptosis. Despite its side effects, cisplatin remains a crucial component of first-line treatments and is also used for patients with recurrent or metastatic cancer. While cisplatin is initially effective at destroying cancer cells, resistance to the drug eventually develops [10]. Cells resist cisplatin through various mechanisms, such as altering drug accumulation by reducing its uptake or increasing efflux. Additionally, they can neutralize the drug via redox-based detoxification, repair the cisplatin-induced DNA damage using excision repair pathways, or downregulate the apoptotic processes that the drug typically triggers [11]. Today, cancer treatment options include chemotherapy and radiotherapy, but plant-based phytotherapy also significantly contributes to cancer management. Phytotherapy can enhance the effectiveness of conventional treatments and may help mitigate side effects [12].

Sargassum ilicifolium (Turner) C. Agardh, a member of the *Sargassaceae* family, is a brown seaweed notable for its diverse biochemical constituents. This alga contains essential photosynthetic pigments, including chlorophyll and carotene. It also possesses a range of other compounds, such as steroids, terpenoids, mannitol, polysaccharides, and alginic acid. Additionally, its cell walls are rich in algin, and the cells feature plastids with thylakoidal lamellae, which are crucial for photosynthesis [12]. Fucoidan, a sulfated polysaccharide rich in fucose from brown algae like Sargassum, exhibits diverse biological activities, including antitumor, antioxidant, anti-inflammatory, anticoagulant, antiviral, and immune-regulating properties. Similarly, sodium alginate, derived from alginic acid and found in the cell walls, is valued in the food and pharmaceutical industries for its gelation and hydrophilic properties [13].

In vitro and *in vivo* studies on the ethyl acetate fraction (ETF) of brown algae *S. ilicifolium* demonstrated significant immunostimulatory effects on human

neutrophils. Testing across concentrations from 10 to 100 μg/ml, the ETF notably enhanced chemotaxis, phagocytosis, and intracellular killing activities, particularly at 100 μg/ml. These findings highlight *S. ilicifolium*'s potential as a potent immunomodulator [14]. Fucoidans extracted from *Sargassum ilicifolium* show significant potential in inhibiting oxidative stress and gastric cancer pathogenesis in rats. The protective effects observed, including the improvement in mitochondrial structure, suggest that these benefits may be due to the high sulfate content in the fucoidans [15]. Phlorotannins, marine polyphenols abundant in brown seaweeds, enhance chemotherapy by promoting cancer cell apoptosis while protecting normal cells. When combined, phlorotannin (dieckol)-rich extracts from *Ecklonia cava* and cisplatin amplify apoptosis through increased reactive oxygen species (ROS) and inhibition of the Akt/NF-κB pathway. Additionally, these extracts help prevent cisplatin-induced kidney cell damage [16].

This study aims to evaluate and compare the anti-proliferative and anti-inflammatory effects of purified fucoidan and alginate extracted from *Sargassum ilicifolium* with the effects of the chemotherapeutic drug cisplatin on the MDA-MB-231 breast cancer cell line, a model for TNBC.

2. Materials and methods

2.1 Materials

The MDA-MB 231 human breast cancer cell line was supplied by the National Cell Bank of Iran (Pasteur Institute of Iran, Tehran, Iran). 2,2-Diphenyl-1-picrylhydrazyl (DPPH) polycaprolactone (PCL) (80,000 Mn), 2,4,6-Tri (2-pyridyl)-s-triazine (TPTZ), ammonium persulfate ($(NH_4)_2\ S_2O_8$), *In vitro* Toxicology Assay Kit (XTT based), penicillin-streptomycin and butylated hydroxyanisole (BHA) were purchased from Sigma Aldrich™ (USA). Roswell Park Memorial Institute (RPMI) and fetal bovine serum (FBS) were purchased from GIBCO™ (USA). Acrylamide was purchased from Pharmacia™ (USA). The Total RNA Isolation kit (Hybrid RTM) was purchased from GeneAll™ (South Korea). SYBR® Premix Ex Taq (Tli RNase H Plus) was purchased from Takara Bio™ (Japan). High Capacity cDNA Reverse Transcription Kit was purchased from Applied Biosystems™ (USA). Pierce bicinchoninic acid (BCA) Protein Assay Kit was purchased from Thermo scientific™ (USA). Agarose gel, ethanol 96%, acetic acid (CH_3COOH), trypsin-ethylene diamine tetra acetic Acid (EDTA), and tetramethylethylenediamine (TEMED), Triton X-100, and Tris were purchased from Merck™ (Germany). All other chemicals and solvents were of the highest grade commercially available.

2.2 Sample preparation

S. ilicifolium was collected from the Persian Gulf Beach in Hormozgan province, Iran. The Taxonomy Laboratory at the Faculty of Pharmacy, Mazandaran University of Medical Science, Iran, identified and confirmed the sample to ensure accurate taxonomic classification. The brown algae were meticulously cleaned to remove epiphytes, waste, and necrotic tissue. After rinsing with fresh water, the algae were sun-dried and placed in an oven at 40°C for 2 days to ensure thorough dehydration. Then, a freeze dryer (Christ™, Germany) was employed at −20°C for 3 days. The dried algae were then finely cut and ground into a fine powder using a mixer grinder

(Yazicilar™, Turkey). The resulting powder was stored in a dry, clean, and sealed container to maintain its integrity.

2.3 Extraction and purification of sodium alginates

Alginate extraction from *S. ilicifolium* was conducted following a high-temperature alkaline extraction method, according to Bouissil et al. Initially, 85 grams of depigmented and dried algae were subjected to two rounds of treatment with 500 ml of 0.1 M HCl at 60°C, maintaining a pH of 2.0 with continuous stirring (Drawell™, China) at 250 rpm for 2 hours. The mixture was centrifuged (Kaida™, China) at 5000 rpm for 15 minutes at 4°C. The resulting residue, or pellet, was rinsed with distilled water and subsequently treated with a 3% w/v solution of sodium carbonate (Na_2CO_3) at pH 11.0 for 2 hours at 60°C, again under constant stirring. The supernatants from this process were collected and precipitated using three volumes of ice-cold 96% ethanol. The precipitate was further centrifuged and resuspended in distilled water before being acidified with 6 M HCl to a pH below 3.0, precipitating alginic acid. This acid was then redissolved in distilled water and neutralized to pH 7.5. The final purification of alginates involved three successive precipitations using ice-cold 96% ethanol. The resulting precipitate was resuspended in distilled water and lyophilized to produce powdered sodium alginates from *S. ilicifolium* algae [17].

2.4 Extraction and purification of fucoidan

Since fucoidans are polar, hydrophilic, and water-soluble macromolecules, water is an excellent solvent for their extraction. Fucoidan was extracted from 180 g of *S. ilicifolium* powder using 40 ml of water heated to 70°C. The extract was then purified through ethanol precipitation. To further remove alginate, 1.5 ml of 3 M $CaCl_2$ was added. Lipids and pigments were effectively eliminated using a solvent mixture of acetone and diethyl ether. Finally, the sediment was dried at 40°C for 24 hours, yielding a concentrated fucoidan extract [18, 19].

2.5 Preparation of polysaccharides from the algae

About 10 g of dried and finely *S. ilicifolium* algae was subjected to extraction using distilled water heated to 90°C in a water bath for 3 hours. Following this initial extraction, the mixture was filtered, and the remaining solid residue underwent a second extraction using distilled water under the same conditions for another 3 hours. The combined extracts were then centrifuged to eliminate any impurities. The clear supernatant obtained from this process was concentrated using rotary evaporation to refine the extract further [20].

2.6 Total carbohydrate determination

The phenol-sulfuric acid method was used to quantify the total carbohydrate content in polysaccharides. In this procedure, 2.5 ml of 96% sulfuric acid was added to 10 μL of the sample at a concentration of 1 mg/ml and to a series of standard glucose solutions ranging from 5 to 200 μg/ml. Then, 500 μL of a 4% phenol solution was quickly added into each tube. The resulting mixture was then incubated in a water bath at 90°C for 5 minutes. A standard curve was created using various concentrations of D-glucose to ensure accurate quantification [21].

2.7 Structural analysis of fucoidan and alginate

The UV–Vis absorbance spectrum of alginate extracted from *S. ilicifolium* was measured using a Double Beam T80 series spectrophotometer (PG Instruments™, China) across the 200–800 nm wavelength range. To analyze the composition and block structure of the extracted alginate, ^{1}H NMR spectroscopy was employed, with the alginate sample prepared at a concentration of 6 mg/ml in deuterium oxide (D_2O). For infrared (IR) analysis, the dried alginate sample was finely ground and mixed with anhydrous potassium bromide (KBr) to form pellets. The IR spectra were then recorded at room temperature, covering a frequency range of 650–4000 cm^{-1} using a Fourier-transform infrared (FTIR) spectrometer [22].

2.8 Determination of antioxidant capacity

2.8.1 DPPH assay

The DPPH assay is a widely used technique to assess the radical-scavenging potential of various compounds. DPPH exhibits a deep purple color in its stable form, which diminishes when it interacts with antioxidants that donate electrons to neutralize the free radicals. In this assay, 8 mg of a DPPH solution is mixed with 100 ml of methanol, and 2 ml of the test extract is added at various concentrations alongside ascorbic acid as a reference antioxidant. The mixtures are then incubated in the dark at room temperature for 30 minutes to allow the reaction to occur. After incubation, the absorbance of the solutions is measured at 517 nm. The inhibition percentage of the DPPH radical is determined using the following formula:

$$\text{Scavenging rate} = \left(\left(A_0 - A_S \right) / A_0 \right) \times 100 \quad (1)$$

A_0 represents the absorbance of the DPPH solution without the sample, and A_S is the absorbance with the sample present. The IC_{50} value, indicating the concentration required to neutralize 50% of the DPPH radicals, is then calculated from the standard curve [23].

2.8.2 Measurement of FRAP

Total antioxidant activity was assessed using the FRAP (ferric reducing ability of plasma) method, which measures the reduction of ferric ions (Fe^{3+}) to ferrous ions (Fe^{2+}) by antioxidants present in biological samples. In this procedure, 50 μL of serum was combined with 1.5 ml of FRAP reagent, prepared from 25 ml of 300 mM acetate buffer (pH 3.6), 2.5 ml of 10 mM TPTZ solution in 40 mM HCl, and 2.5 ml of 20 mM $FeCl_3$. The mixture was vortexed to ensure thorough mixing and then incubated at 37°C in a water bath for 5 minutes. The reaction's progress was monitored by measuring the absorbance at 593 nm, which corresponds to the formation of the Fe^{2}-TPTZ complex. A standard curve was generated using stock solutions of $FeSO_4 \cdot 7H_2O$ to quantify antioxidant activity at concentrations of 125, 250, 500, 750, and 1000 μM. The results were expressed as mM of Fe^{2+} per gram of dried mass [24].

2.9 Cell culture

MDA-MB 231 cells were cultured in RPMI-1640 medium enriched with 10% heat-inactivated fetal bovine serum (FBS), 100 IU/ml penicillin, and 100 μg/ml streptomycin. The cultures were maintained in a controlled environment at 37°C with 5%

CO_2 to ensure optimal growth conditions. The cells were subcultured twice weekly, starting at approximately 5×10^5 cells/ml density. Cell viability was assessed using the trypan blue exclusion method, which selectively stains non-viable cells, allowing for accurate viability measurements [25].

2.9.1 Cryopreservation of MDA-MB-231 cells

Cryopreservation is a critical method used to preserve the viability and functionality of cell lines for extended durations. The procedure begins by harvesting cells during their logarithmic growth phase. This is achieved by detaching the cells from the culture flask using 0.25% trypsin and EDTA. The detached cells are then washed with RPMI-1640 medium to remove residual trypsin and other impurities. The cells are counted using a hemocytometer to assess cell viability and concentration. Subsequently, 3 million cells are transferred into conical tubes and subjected to centrifugation at 1500 rpm for 5 minutes. After centrifugation, the supernatant is carefully discarded, leaving behind the cell pellet thoroughly resuspended in a suitable buffer. For each 3 million cells, 1 milliliter of freezing medium is added to cryovials. The vials are then cooled at a controlled rate, typically 1°C per minute, using a specialized freezer container (Mr. Frosty™, USA) down to −20°C for 1 hour. Subsequently, the vials are transferred to a −70°C freezer for 24 hours. Finally, the cryovials are stored in liquid nitrogen tanks for long-term preservation. Each cryovial is meticulously labeled with key information, including the cell type, date of freezing, and passage number [26].

2.9.2 Thawing procedure for cryopreserved cells

The thawing protocol is critical for the successful recovery of cryopreserved cells, ensuring they are viable for future experiments and applications in cell culture studies. Unlike the slow freezing process, thawing must be done quickly to avoid cellular damage from dimethyl sulfoxide (DMSO). The process begins with preparing the necessary equipment and culture medium under sterile conditions. Cryovials containing frozen cells are swiftly removed from liquid nitrogen storage and immersed in a 37°C water bath. This rapid thawing process is carefully monitored, with attention to the melting of DMSO, which has a higher freezing point. Once the ice crystals have fully dissolved, the cells are quickly transferred to a sterile conical tube containing RPMI medium supplemented with 10% FBS. The tube is then centrifuged at 1500 rpm for 5 minutes at room temperature to separate the cells from the residual DMSO. The supernatant, now containing the DMSO, is gently discarded to preserve the integrity of the cell pellet. Cell counting and viability assessments are then performed, typically using trypan blue exclusion or automated cell counting methods. The viable cells are seeded at the appropriate density into a T25 flask (SPL™, South Korea) containing a medium with 10% FBS. After a 24-hour incubation period, the culture medium is replaced to remove any remaining DMSO, and the cell's morphology is assessed using an inverted microscope.

2.10 Cytotoxicity evaluation of fucoidan, sodium alginates, and cisplatin on MDA-MB-231 cancer cells

To assess their response, MDA-MB-231 cell lines were exposed to a range of fucoidan (0–800 μg/ml), sodium alginates (0–350 μg/ml), and cisplatin (0–20 μg/ml)

concentrations. IC50 was determined using the 2, 3-bis-(2-methoxy-4-nitro-5-sulfophenyl)-2H-tetrazolium-5-carboxanilide (XTT) colorimetric assay, which measures cell viability based on metabolic activity. In the experiment, 2×10^4 MDA-MB-231 cells were seeded into each well of a 96-well plate, followed by adding 0.1 ml of medium containing different concentrations of fucoidan, sodium alginates, and cisplatin. After incubating the cells for 48 hours at 37°C in a 5% CO_2 atmosphere, the XTT reagent was introduced to each well. The absorbance was then measured at 450 and 620 nm using a multifunctional ELISA reader. To ensure the reliability of the results, all experiments were repeated three times to ensure accuracy [27].

2.11 Drug interaction analysis in MDA-MB-231 cells

The analysis of drug interactions was conducted using CompuSyn software, which utilizes the modified Chou-Talalay Combination Index (CI) method. This software helps calculate the required doses of drugs, individually and in combination, to achieve specific levels of cytotoxicity. The software calculates a Combination Index (CI) for each cytotoxicity level to evaluate the drug interaction. In the study, MDA-MB-231 cells were treated with 3.6 μg (IC_{20}) of cisplatin and various concentrations of fucoidan and sodium alginates-rich extract to assess the interactions. The CI values were used to determine the type of interaction: synergistic (CI < 1), additive (CI = 1), or antagonistic (CI > 1).

The outcomes of these interactions were visualized using several plots:

i. *Dose-effect curve*: This plot shows the dose-response relationship for both the drug and the extract, individually and in combination.

ii. *Fa-CI plot*: It differentiates between antagonism (CI > 1) and synergism (CI < 1) based on the Combination Index.

iii. *Median-effect plot*: This plot illustrates the relationship between the drug dose (Log D) and the effect (Log Fa/Fu). The IC_{50} value is identified where the curve intersects the X-axis.

iv. *Dose-normalized isobologram*: Points on this plot show the interaction between the drug and the extract, indicating synergism, antagonism, or an additive effect based on their position relative to the diagonal line [28].

2.12 Measurement of IL-1 and IL-6 from a THP-1 monocyte cell line stimulated with bacterial lipopolysaccharide (LPS) and treated with non-toxic concentrations of an alginate and fucoidan-rich extract

Human acute monocytic leukemia cells (THP-1) supplied by Pasteur Institute of Iran were cultured in RPMI 1640 medium with 10% fetal bovine serum and 100 μM penicillin-streptomycin under conditions of 95% air and 5% CO_2. In the experiment, 4×10^4 Differentiated THP-1 cells were seeded into each well of a 96-well plate and then exposed to 1 μg/ml of bacterial LPS for 24 hours along with concentrations of 5 and 50 μg/ml of fucoidan-rich extract and with concentrations of 25 and 250 μg/ml of alginate-rich extract given in duplicate for each cultured sample. After 48 hours, the cells were collected, and the supernatants were stored at −20°C for cytokine analysis. The cell pellets were washed with phosphate-buffered saline (PBS), centrifuged at

1000 rpm for 8 minutes, and then stored at −20°C. According to the manufacturer's instructions, IL-1 and IL-6 levels were evaluated using commercially available ELISA kits [29].

2.13 Cytotoxicity evaluation of alginate and fucoidan-rich extract in a 3D culture model

The fabrication and design of the nano-scaffold were performed using an electrospinning device (Fanavaran Nano Meghyas™, Iran). The setup involved an injection flow rate of 1 ml/h, a needle distance of 15 cm, and a total volume of 10 ml. The structural characteristics of the Electrospun Polycaprolactone (PCL) nano-scaffolds were analyzed using scanning electron microscopy (SEM), which provided detailed visualization of the fiber alignment and diameter. To improve the surface properties of the PCL nanofibers, they were treated with O_2 plasma to increase hydrophilicity. This modification was performed for 5 minutes at a pressure of 0.4 millibars and a power of 30 W in a microwave plasma chamber. The plasma treatment was critical for enhancing cell adhesion and proliferation by making the nanofiber surface more wettable. For sterilization, the PCL nanofibers were treated with 70% ethanol, eliminating microbial contaminants. Post-sterilization, the nanofibers were rinsed three times with phosphate-buffered saline (PBS) to remove any ethanol residues. The nanofibers were then freeze-dried, preserving the scaffold's structural integrity while maintaining its mechanical properties. Combining SEM analysis, plasma surface modification, ethanol sterilization, and freeze-drying produced high-quality PCL nano-scaffolds ideal for applications in 3D cell culture [30].

2.14 Cytotoxicity evaluation of fucoidan-rich extract and cisplatin on MDA-MB-231 cells in a PCL polymeric nano-scaffold

After determining the IC_{50} values for both the fucoidan-rich extract and cisplatin in prior experiments, the cells were treated with varying concentrations—ranging from 0 to 1000 μg/ml of the fucoidan-rich extract and 2.1 μM of cisplatin—under conditions that closely resemble the physiological environment. 3×10^4 cells were seeded into each well of a 96-well plate and allowed to adhere to a polymeric scaffold for 24 hours. Subsequently, different concentrations of the extract and paclitaxel were added in triplicate to each well. An equivalent volume of PBS was added in triplicate for the negative control. The cells were incubated for 48 hours at 37°C with 5% CO_2. Following incubation, cell viability was assessed using the XTT assay, with absorbance readings taken at 450 and 620 nm using an ELISA reader. The entire experiment was conducted three times to ensure reproducibility and accuracy [31].

2.15 Data analysis and statistics

Results are expressed as the mean ± standard deviation (SD). Statistical analyses were conducted utilizing GraphPad Prism version 6 and SPSS version 16. The Kolmogorov-Smirnov test was applied to assess the normality of data distribution. For analyzing the data, paired t-tests were used for normally distributed variables, while the Wilcoxon signed-rank test was employed for non-parametric data. A P-value <0.05 was considered statistically significant in all analyses.

3. Results

3.1 Total sodium alginates and fucoidan determination

The extraction yields of fucoidan and alginate from the dried algae extract were determined to be 7203 and 441 mg per 100 grams of dried extract, respectively. This indicates that 7.2% of the algae extract's dried weight consisted of fucoidan, while 0.44% was alginate.

3.2 Total carbohydrate determination

The polysaccharide fraction from *S. ilicifolium* was obtained through a series of processes, including hot water extraction, ethanol precipitation, and dialysis. Using a calibration curve ($y = 0.0621x + 0.0084$, $r^2 = 0.999$) in absorbance of 490 nm created with standard glucose solutions, the total polysaccharide content in the fraction was estimated to be 89.39 mg/g dried algae weight.

3.3 Antioxidant properties of fucoidan and alginate

3.3.1 FRAP assay

In the reducing power assay, antioxidants present in the samples facilitate the conversion of ferric ions (Fe^{3+}) to ferrous ions (Fe^{2+}) through electron donation. Based on the standard curve equation ($y = 0.6685x + 0.0005$, $r^2 = 0.99$), the quantities of iron reduced by alginate and fucoidan-rich extract of *S. ilicifolium* are detailed in **Table 1**, suggesting higher antioxidant properties in fucoidan-rich extract compare to alginate-rich extract.

3.3.2 DPPH assay

The IC_{50} value for DPPH was assessed for different concentrations of algae's fucoidan-rich and alginate-rich extracts. The calculations were based on the standard curve equation ($y = 14.497x + 28.764$, $r^2 = 0.9962$) for ascorbic acid as a reference antioxidant.

For fucoidan, the standard curve equation was ($y = 21.35x + 0.1283$, $r^2 = 0.9955$), which exhibited a 33.9% inhibition at a concentration of 100 μg/ml as the highest percentage of inhibition with IC_{50} of 180.6 ± 26.3 μg/ml.

For alginate, the standard curve equation was ($y = 1.3217x + 0.076$, $r^2 = 0.9976$), which demonstrated a 16.7% inhibition at a concentration of 200 μg/ml as the highest percentage of inhibition, with IC_{50} of 640 ± 37.4 μg/ml.

Extract	FRAP at Concentration 0.1 mg/ml	FRAP at Concentration 1 mg/ml
Fucoidan-rich	153.6 ± 8.4 (μg/ ml)	865.5 ± 23.2 (μg/ ml)
Alginate-rich	43.8 ± 3.7 (μg/ ml)	105.3 ± 9.4 (μg/ ml)

Table 1.
The ferric-reducing ability of plasma of different concentrations of fucoidan and alginate-rich extract of S. ilicifolium.

3.4 FTIR spectrum of sodium alginate

The FTIR spectrum of sodium alginate (**Figure 1**) identified various chemical functional groups. A prominent broad absorption band at 3465 cm^{-1} indicates the hydroxyl group's (–OH) stretching vibrations. Additionally, peaks within the 2845 to 2930 cm^{-1} range correspond to the stretching vibrations of the methylidyne group (–CH). Significant peaks observed within 1599 ± 4 and 1410 ± 4 cm^{-1} are associated with asymmetric and symmetric stretching of carboxylate anions (COO–), respectively. The spectrum also displays a shoulder band at 1083.444 cm^{-1}, reflecting C–C and C–O stretching vibrations, which suggest cross-linking within the alginate structure. Moreover, the peak at 1022.493 cm^{-1} is attributed to C–C stretching vibrations, further characterizing the molecular framework.

3.5 FTIR spectrum of fucoidan

The FTIR spectrum of fucoidan revealed several key chemical functional groups (**Figure 2**). A broad and intense absorption band within the 3000 to 3600 cm^{-1} range signifies the stretching vibrations of hydroxyl groups (–OH), indicative of hydrogen bonding, commonly associated with polysaccharides. Additionally, absorption peaks between 2845 and 2930 cm^{-1} correspond to the stretching vibrations of the methylidyne (–CH) group. Further analysis shows spectral peaks between 1610 and 1651 cm^{-1}, attributed to carbonyl (C═O) and carbon-carbon double bond (C═C) stretching vibrations. These are linked to the presence of uronic acids, suggesting alginic acid as part of the alginate polymers in the sample. Peaks between 1420 and 1445 cm^{-1} are possibly related to C–H deformation or –OH rocking vibrations in monosaccharides. The FTIR spectrum also indicates the presence of C-O-C and C-O-S bonds, with observed peaks ranging from 387 to 1030 cm^{-1}. Specifically, a peak

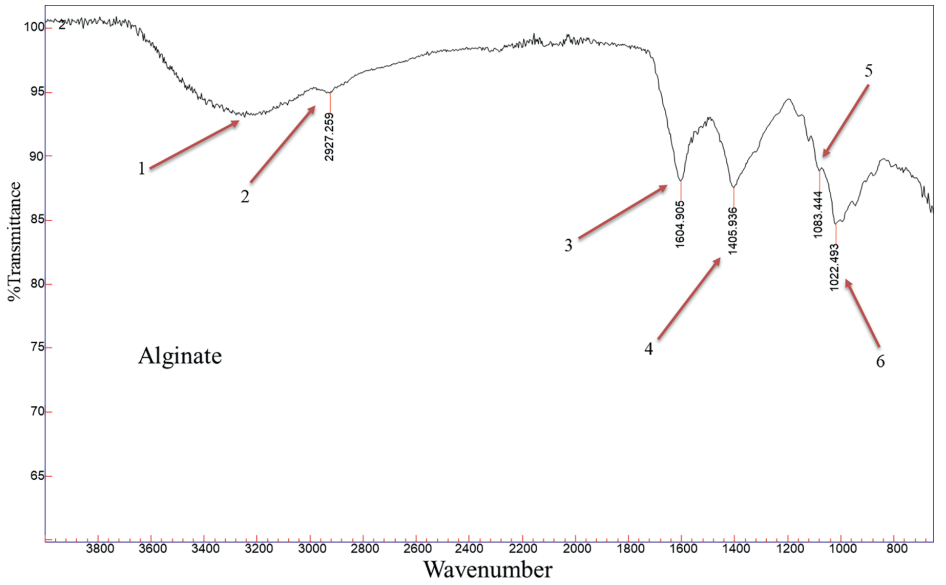

Figure 1.
FTIR analysis of sodium alginate.

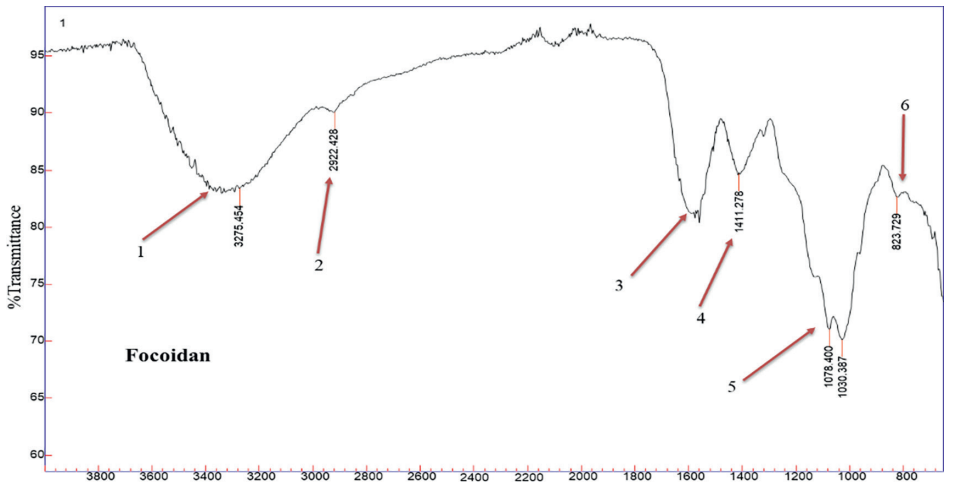

Figure 2.
FTIR analysis of fucoidan.

near 1078.4 cm^{-1} signifies C–O, C–C, and C–O–H stretching vibrations in hydrocarbon structures. Lastly, the sharp absorption bands between 729 and 823 cm^{-1} are attributed to C–O–S bending vibrations, pointing to sulfate substitution.

3.6 UV-visible analysis

The UV-visible spectrogram of the alginate extract (**Figure 3**) displayed absorption peaks within the 200–400 nm range, which are indicative of carboxylate groups and protein-related components. Peaks observed at 280, 370, and 405 nm suggest the presence of phenolic compounds, flavonoids, and their derivatives. The data further highlighted absorption bands between 280 and 410 nm, characteristic of aromatic and polycyclic aromatic compounds, including proteins and amino acids, supporting complex organic structures in the extract.

The spectrogram of the fucoidan extract (**Figure 4**) in the 300 to 400 nm range appears abnormal, possibly due to impurities, sample preparation issues, or instrumental problems. Polysaccharides in their pure form are generally optically

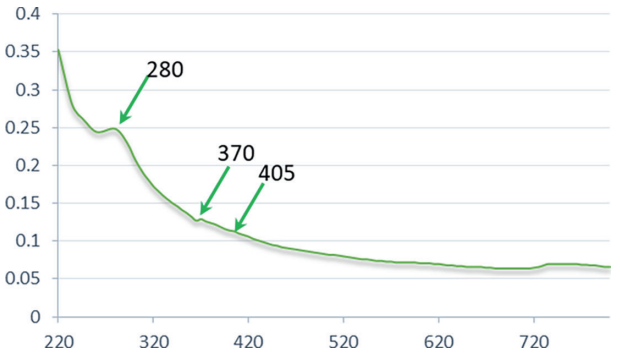

Figure 3.
UV spectrogram of alginate extract.

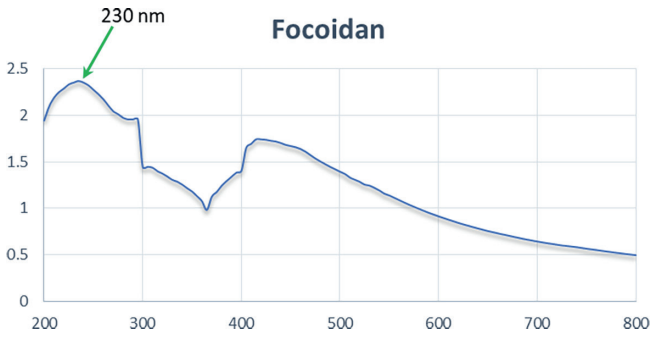

Figure 4.
UV spectrogram of fucoidan extract.

transparent and do not exhibit absorption in the UV-Vis region. The absorption peak around 230 nm may indicate the presence of polyphenols in the sample.

3.7 Cytotoxicity evaluation of cisplatin on MDA-MB-231 cancer cell line

The XTT assay was employed to assess the cytotoxic effects of cisplatin on MDA-MB-231 breast cancer cells. According to the results depicted in **Figure 5**, different concentrations of cisplatin, ranging from 0 to 20 µg/ml, were administered to the cells over 48 hours. Cisplatin demonstrated an evident dose-dependent cytotoxicity, with the IC_{20} and IC_{50} values calculated at 3.6 ± 0.4 and 15.33 ± 0.9 µg/ml, respectively.

3.8 Cytotoxicity evaluation of fucoidan-rich extract and its drug interaction analysis with cisplatin on MDA-MB-231 cancer cell line

The XTT assay was initially conducted to evaluate the impact of a fucoidan-rich extract on the viability of MDA-MB-231 breast cancer cells. As illustrated in **Figure 6** (green line), various extract concentrations, ranging from 0 to 800 µg/ml, were tested over 48 hours. The results revealed that the fucoidan-rich extract induced a dose-dependent cytotoxic effect on the cells, with an IC_{20} value (the

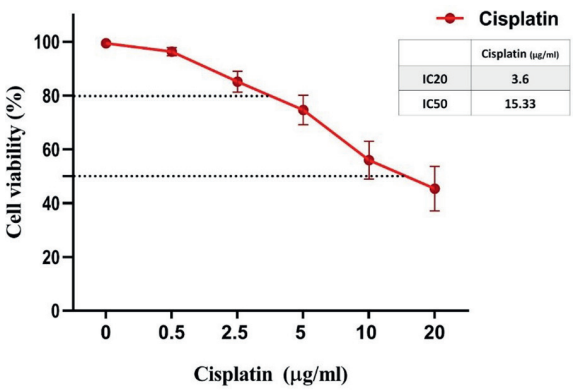

Figure 5.
Cytotoxicity evaluation of different concentrations of cisplatin on MDA-MB-231 cancer cells.

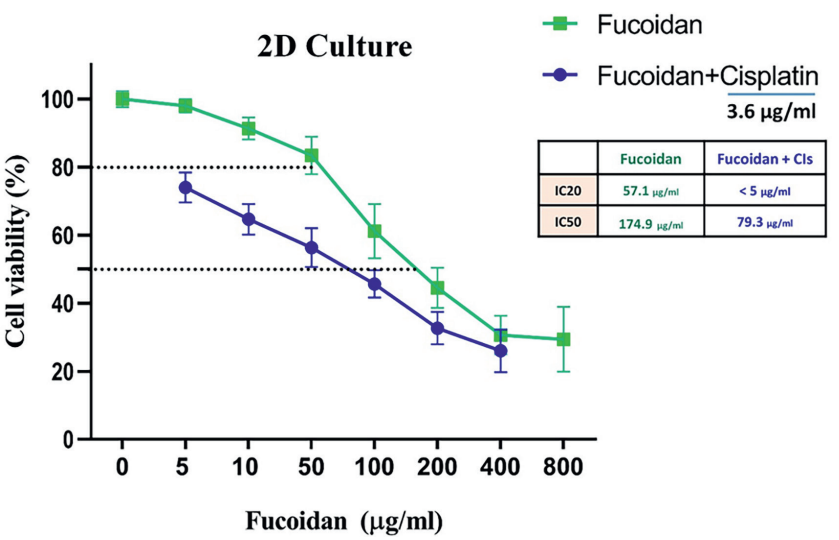

Figure 6.
Cytotoxicity evaluation of fucoidan-rich extract and in combination with cisplatin on MDA-MB-231 cancer cells.

concentration at which 80% of cells remain viable) of 57.1 ± 2.9 µg/ml and an IC_{50} value of 174.9 ± 8.7 µg/ml.

Subsequently, the effects of combining different concentrations of the fucoidan-rich extract (ranging from 5 to 400 µg/ml) with 3.6 ± 0.4 µg/ml (IC_{20}) of cisplatin were analyzed. As shown in **Figure 6** (blue line), after 48 hours of treatment, the combination significantly enhanced cytotoxicity, reducing the IC_{50} from 174.9 ± 8.7 to 79.3 ± 4.6 µg/ml and lowering the IC_{20} from 57.1 ± 2.9 µg/ml to below 5.0 ± 0.8 µg/ml. This indicates a synergistic effect between the fucoidan-rich extract and cisplatin.

The synergistic interaction between the fucoidan-rich extract and cisplatin was validated through CompuSyn software analysis. This software calculated the Combination Index (CI) values for all tested concentrations, with values less than one consistently indicating a synergistic effect (as shown in **Table 2**). Among the tested concentrations, 200 µg/ml demonstrated the highest synergy, with a CI value of 0.28518.

A detailed analysis using CompuSyn software generated several insightful plots (**Figure 7**).

1. *Dose-effect curve* (**Figure 7A**): The combination treatment demonstrated a more substantial dose-dependent effect than the extract alone. The green points, representing the combined treatment of cisplatin and extract, were positioned lower on the graph than the blue line, corresponding to the extract alone. This positioning indicates enhanced cytotoxicity when the treatments are combined.

2. *Combination index plot* (**Figure 7B**): All Fa-CI points fell below the line at 1, signifying synergistic effects at all concentrations tested. This confirms that combining treatments is more effective than either treatment alone.

3. *Median-effect plot* (**Figure 7C**): The log-transformed data revealed positive slope lines, indicating that higher doses correlate with increased cellular response. The point where the lines intersect the X-axis represents the combined IC_{50} value, calculated at 79.3 ± 4.6 µg/ml.

Fucoidan concentration (μg/ml)	CI	Effect
5	0.69302	Synergism
10	0.41359	Synergism
50	0.47320	Synergism
100	0.38466	Synergism
200	0.28518	Synergism
400	0.32998	Synergism

Table 2.
Combination index of different concentrations of fucoidan-rich extract in combination with IC_{20} concentration (3.6 ± 0.4 μg/ml) of cisplatin.

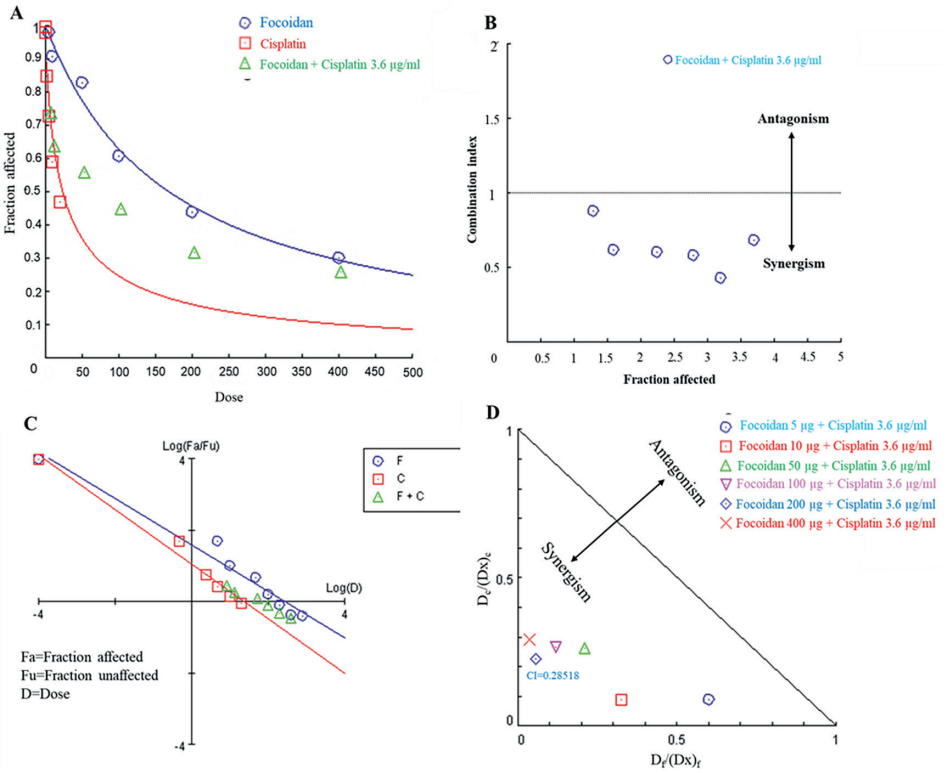

Figure 7.
Plot analysis of fucoidan-rich extract and cisplatin on MDA-MB-231 cells using CompuSyn software. (A) Dose-effect curve (B) Combination index plot (C) Median-effect plot (D) Dose-normalized isobologram.

4. *Dose-normalized isobologram* (**Figure 7D**): This plot demonstrated that all combined doses, represented by colored points within the triangle, displayed synergistic effects, with CI values consistently below one, reinforcing the enhanced effectiveness of the combination therapy. The colored points represent the concentration of the combined drug. The closer a point is to the left and bottom, the lower its CI number and the more potent its synergistic effect. Since all five concentrations combined with cisplatin fall within the triangle, each concentration demonstrates a synergistic effect with a CI of less than one.

3.9 Cytotoxicity evaluation of alginate-rich extract and its drug interaction analysis with cisplatin on MDA-MB-231 cancer cell line

As mentioned for fucoidan-rich extract, the XTT assay was used to assess the effects of an alginate-rich extract on the viability of MDA-MB-231 breast cancer cells. **Figure 8** (blue line) shows that varying extract concentrations, ranging from 0 to 350 μg/ml, were tested over 48 hours. The findings indicated that the alginate-rich extract exhibited minimal toxicity toward the MDA-MB-231 cell line, with significant cytotoxicity observed only at concentrations exceeding 280 μg/ml, surpassing the IC_{20} threshold.

The combined effects of the various concentrations of alginate-rich extract (ranging from 0 to 350 μg/ml) with 3.6 μg/ml of cisplatin (IC_{20}) were evaluated. As shown in **Figure 8** (green line), after 48 hours of treatment, the combination did not result in any notable increase in cytotoxicity, suggesting that the alginate-rich extract did not enhance the cytotoxic effects of cisplatin in this cell line.

The interaction between the alginate-rich extract and cisplatin was further analyzed using CompuSyn software. The Combination Index (CI) values, calculated across all tested concentrations, revealed that the alginate-rich extract displayed both weak synergistic and antagonistic effects when combined with the IC_{20} concentration of cisplatin (**Table 2**). Notably, the 50 μg/ml concentration exhibited the strongest synergy, with a CI value of 0.83198 (**Table 3**).

A detailed analysis using CompuSyn software generated several detailed plots (**Figure 9**).

1. *Dose-effect curve* (**Figure 9A**): The combination of alginate and cisplatin did not increase toxic effects as the alginate concentration was raised. This is evident from the horizontal trend of the green triangles in the dose-effect plot, representing the combination of the alginate extract and cisplatin, which indicates that alginate has an insignificant impact on enhancing cisplatin's toxicity. Moreover, the red line, which denotes the cytotoxic effect of various concentrations of cisplatin alone, demonstrates the potent toxicity of the drug.

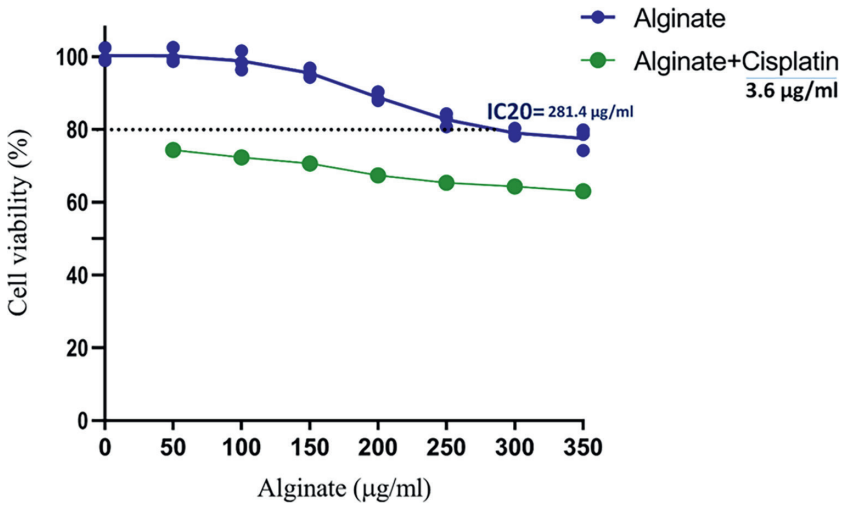

Figure 8.
Cytotoxicity evaluation of alginate-rich extract and in combination with cisplatin on MDA-MB-231 cancer cells.

Alginate concentration (μg/ml)	CI	Effect
50	0.83198	Synergism
100	0.94180	Synergism
150	1.05919	Antagonism
200	1.12509	Antagonism
250	1.22702	Antagonism

Table 3.
CI of different concentrations of fucoidan-rich extract in combination with IC20 concentration (3.6 ± 0.4 μg/ml).

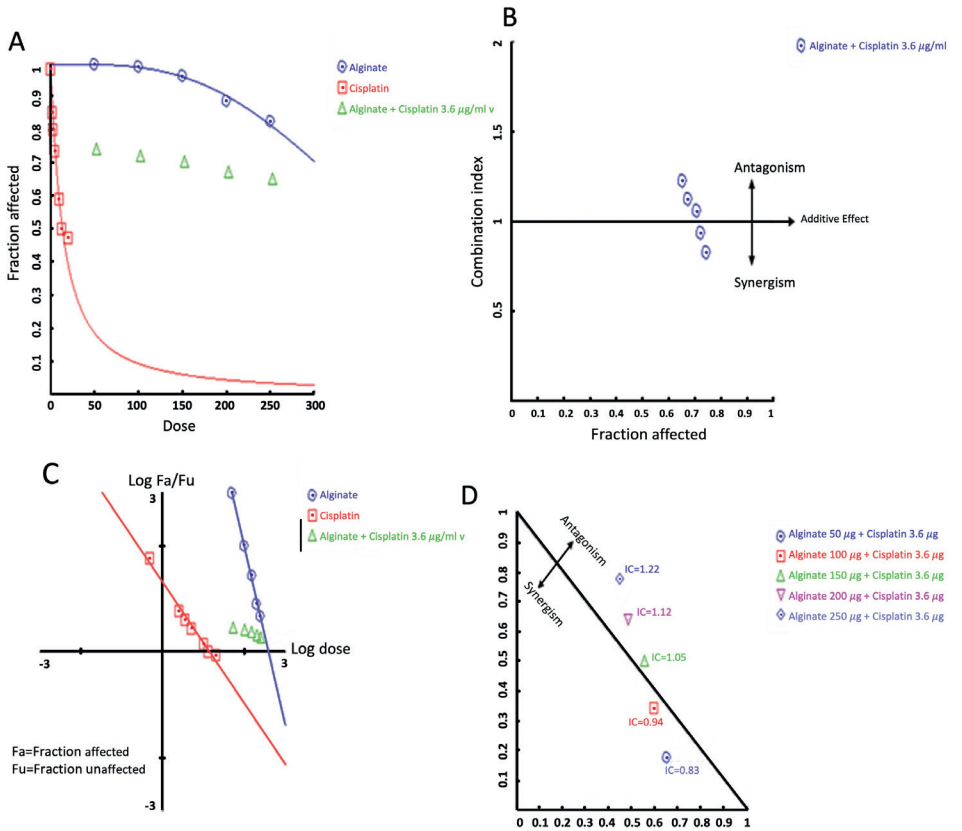

Figure 9.
Plot analysis of alginate-rich extract and cisplatin on MDA-MB-231 cells using CompuSyn software. (A) Dose-effect curve (B) Combination index plot (C) Median-effect plot (D) Dose-normalized isobologram.

2. *Combination index plot* (**Figure 9B**): In the Fa-CI diagram, two data points fell below the line, indicating a synergistic interaction at these two concentrations. However, an antagonistic interaction occurs at three other concentrations of Fa-CI points positioned above the line at 1.

3. *Median-effect plot* (**Figure 9C**): The log-transformed data revealed that increasing the dose does not lead to a significant rise in cytotoxic response due to the shallow slope of the combination curve for the drug and the extract. This indicates that the

tested alginate concentrations did not reach the IC_{50} threshold. Furthermore, the combination of alginate with cisplatin also failed to achieve an IC_{50}, reflecting the limited enhancement in cytotoxicity when these two agents are used together.

4. *Dose-normalized isobologram* (**Figure 9D**): Doses represented within the triangle display a synergistic effect when combined with cisplatin, while the doses plotted outside the triangle exhibit antagonistic effects. The colored points represent the concentration of the combined drug. The closer a point is to the left and bottom, the lower its CI number and the more potent its synergistic effect. Two concentrations, which lie inside the triangle and close to the diagonal line, show only a weak synergistic effect. In contrast, three concentrations situated outside the triangle demonstrate antagonistic interactions.

3.10 IL-1β and IL-6 cytokine secretion from THP-1 monocyte cell line stimulated with *S. ilicifolium* fucoidan-rich extract

The impact of non-toxic doses (5 and 50 μg/ml) of *S. ilicifolium* fucoidan-rich extract on cytokine secretion was evaluated using the THP-1 monocyte cell line. Lipopolysaccharide (LPS, 1 μg/ml) was used as a positive control to stimulate cytokine secretion. The results revealed that, compared to the untreated control group, both the 5 and 50 μg/ml doses of the extract significantly reduced IL-1β cytokine secretion by 14% (p-values = 0.0411) and 37% (p-values = 0.0022), respectively (**Figure 10**).

Similarly, for IL-6 cytokine, the 5 and 50 μg/ml doses of the extract led to significant reductions of 16% (p-values = 0.0411) and 42% (p-values = 0.0022), respectively, as shown in **Figure 11**.

3.11 IL-1β and IL-6 cytokine secretion from THP-1 monocyte cell line stimulated with *S. ilicifolium* alginate-rich extract

The effect of non-toxic doses (50 and 250 μg/ml) of *S. ilicifolium* alginate-rich extract on cytokine secretion was assessed using the THP-1 monocyte cell line, with

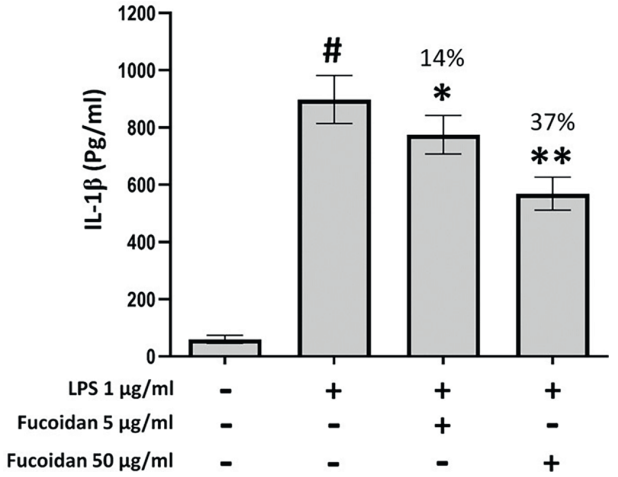

Figure 10.
The effect of non-toxic doses of S. ilicifolium *fucoidan-rich extract on the secretion of IL-1β cytokine from THP-1 monocyte cell line, # control group, * and ** P value<0.05 compared to the control group.*

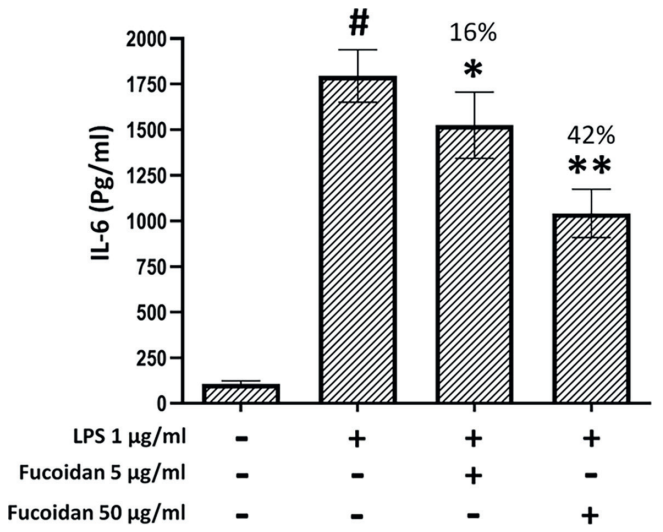

Figure 11.
The effect of non-toxic doses of S. ilicifolium *fucoidan-rich extract on the secretion of IL-6 cytokine from THP-1 monocyte cell line, # control group, * and ** P value<0.05 compared to the control group.*

lipopolysaccharide (LPS, 1 µg/ml) serving as a positive control to induce cytokine production. The findings indicated that, compared to the untreated control group, both the 50 and 250 µg/ml concentrations of the extract significantly decreased IL-1β cytokine secretion by 8 and 15%, with p-values of 0.0411 and 0.0022, respectively (**Figure 12**).

Similarly, the extract significantly reduced IL-6 cytokine levels by 5 and 13% at doses of 50 and 250 µg/ml, with corresponding p-values of 0.0411 and 0.0022, as depicted in **Figure 13**.

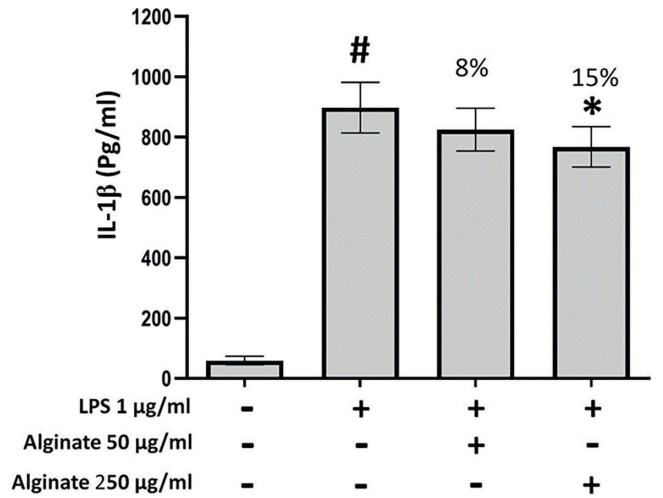

Figure 12.
The effect of non-toxic doses of S. ilicifolium *alginate-rich extract on the secretion of IL-1β cytokine from THP-1 monocyte cell line, # control group, * and ** P value<0.05 compared to the control group.*

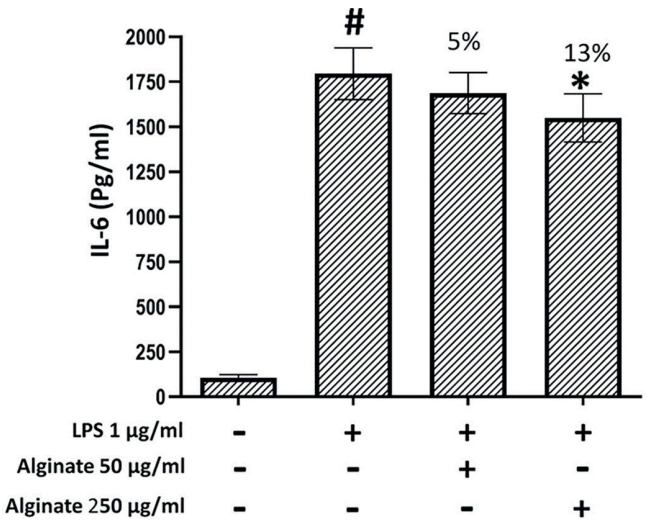

Figure 13.
The effect of non-toxic doses of S. ilicifolium *alginate-rich extract on the secretion of IL-6 cytokine from THP-1 monocyte cell line, # control group, * and ** P value<0.05 compared to the control group.*

3.12 Cytotoxicity evaluation of fucoidan-rich extract on cancer cells and its drug interaction analysis with paclitaxel on MDA-MB-231 cell line in a PCL polymeric nano-scaffold

Cell viability was measured using the XTT assay across a range of extract concentrations to assess the cytotoxic potential of a fucoidan-rich extract on MDA-MB-231 breast cancer cells. As depicted in **Figure 14** (green line), after 48 hours of treatment with concentrations between 0 and 800 µg/ml, the extract exhibited evident

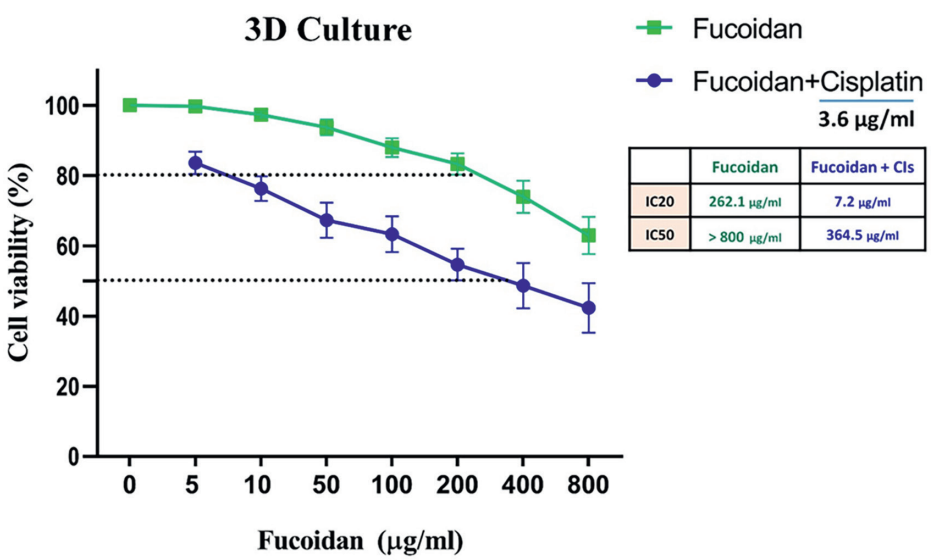

Figure 14.
Cytotoxicity evaluation of fucoidan-rich extract in combination with cisplatin on MDA-MB-231 cells in a 3D culture model.

dose-dependent cytotoxicity against MDA-MB-231 cells. The IC_{20}, or the concentration required to inhibit 20% of cell growth, was calculated at 262.1 ± 19.7 μg/ml, while the IC_{50} exceeded 800 ± 78.5 μg/ml.

Furthermore, as shown in **Figure 14** (blue line), the cytotoxic effect was notably enhanced when the extract was combined with 3.6 μg/ml cisplatin for 48 hours. The IC_{20} dropped sharply from 262.1 ± 19.3 to 7.2 ± 1.4 μg/ml, and the IC_{50} decreased significantly from over 800 ± 78.5 to 364.5 ± 41.7 μg/ml.

4. Discussion

Breast cancer remains a significant global public health challenge and stands as the most prevalent cancer among women. Predictions estimate that by 2040, the global incidence of breast cancer will exceed 3 million new cases annually, accompanied by nearly 1 million deaths each year. Among the various subtypes, triple-negative breast cancer (TNBC) is particularly aggressive, known for its high mortality rates and a pronounced tendency to metastasize beyond the breast to distant organs. This makes TNBC one of the most challenging forms of breast cancer to treat and underscores the urgent need for improved therapeutic strategies [32, 33]. The application of immunostimulants, particularly as adjuvants to chemotherapy, offers significant potential for controlling and preventing cancers. There is growing interest in exploring bioactive compounds from marine-derived drugs as immunomodulatory agents in alternative medicine [14]. This study evaluated the fucoidan and alginate-rich extract of *S. ilicifolium* for their potential impact on immune function along with cisplatin as a chemotherapeutic agent, highlighting their promise in enhancing immune response and supporting therapeutic interventions.

The antioxidant, cytotoxic, and apoptotic properties of fucoidan and alginate from the brown algae *Colpomenia sinuosa* have shown promising anticancer effects across various cancer cell lines. Notably, highly sulfated fucoidans exhibited more potent antioxidant and cytotoxic activities than alginate. Human colon cancer cells were susceptible to these treatments, with fucoidan demonstrating a lower IC_{50} value (618.9 μg/ml) than alginate (690 μg/ml). The treatment of HCT-116 cells with fucoidan and alginate from *C. sinuosa* led to a significant increase in reactive oxygen species (ROS) production. This elevated ROS production indicates that these compounds may induce oxidative damage within the cells, which can ultimately trigger cell death through oxidative stress mechanisms. Moreover, when combined with vitamin C, the algal polysaccharides significantly enhanced nuclear degeneration and increased the $subG_1$ cell population, indicating induced cell death [34].

S. ilicifolium, a seaweed native to the coastal regions of the Persian Gulf, is rich in polysaccharides like fucoidan, which exhibit potential anticancer properties, explored through various assays, including MTT, cell culture, viability, and apoptosis tests. The findings demonstrated that within 24 hours, cell viability decreased by 2% at 1 mg/mL of the fucoidan-rich extract, while concentrations of 60 mg/mL reduced cell viability by less than 30%, with an IC_{50} between 20 and 30 mg/ml. Additionally, ELISA results confirmed that the extract induced apoptosis in cancer cells [35].

Fucoidan, a sulfated polysaccharide from brown algae, exhibits various biological activities, including antitumor effects. *In vitro* investigation of fucoidan's crude impact on mouse breast cancer significantly reduced the viability of 4 T1 cells, induced apoptosis, and downregulated VEGF expression. It also decreased Bcl-2 expression, lowering the Bcl-2/Bax ratio, and reduced levels of Survivin and

phosphorylated ERKs. Additionally, fucoidan triggered cytochrome C release from mitochondria and increased cleaved Caspase-3 levels. *In vivo*, intraperitoneal fucoidan injections in breast cancer models reduced tumor volume and weight, enhancing antitumor effects by decreasing angiogenesis and increasing apoptosis [36].

The difference in antioxidant performance between fucoidan and sodium alginate can be attributed to their distinct chemical structures. Both fucoidan and sodium alginate exhibit strong binding affinities to lead, which enables them to restore antioxidant enzyme activity and mitigate oxidative damage by absorbing lead *in vivo*. While sodium alginate is known to have a superior lead adsorption capacity compared to fucoidan, the latter demonstrates greater antioxidant properties. This is likely due to the presence of sulfhydryl groups in fucoidan, which have a strong ability to neutralize excessive free radicals generated by lead-induced toxicity. This unique structural feature of fucoidan may explain its enhanced antioxidant performance in this study, despite both compounds showing similar efficacy in repairing lead-induced oxidative damage in rats [37].

The anticancer effects of fucoidan on human breast cancer MCF-7 cells include inhibition of proliferation and induction of apoptosis in adult Sprague–Dawley rats treated with fucoidan (200 or 400 mg/kg daily) for 3 days show significantly suppressed MCF-7 cell proliferation, enhanced apoptosis, and reduced cell migration and invasion in serum from these fucoidan-treated rats. These effects were linked to the upregulation of E-cadherin and downregulation of MMP-9, suggesting that fucoidan may inhibit the epithelial-mesenchymal transition (EMT) process, thereby reducing cancer cell invasiveness [38]. These results align with our findings and underscore the potential of fucoidan as a potent anticancer agent.

The sodium alginate-curcumin bioconjugate (AA-CUR) shows great potential as an anticancer drug system due to its simple synthesis, high colloidal stability, and effective curcumin release profile. It demonstrates significant cytotoxicity against cancer cells while maintaining low toxicity in normal cells, making it a promising candidate for therapeutic applications [39]. Alginate/lignin is a promising antioxidant material with potential applications in pharmaceuticals, functional foods, and diabetes management. The acute toxicity test of alginate/lignin in mice presented an LD_0 of (3.91 g/kg) and LD_{100} of (9.77 g/kg). It demonstrates strong total antioxidant activity and effective α-glucosidase inhibition, crucial for controlling blood sugar levels. Although it shows minimal effects on cancer cells, its thermal stability, spherical structure, and unique composition of metals and non-metals enhance its suitability for therapeutic uses, particularly in treating aging-related conditions, diabetes, and digestive system disorders. Additionally, its low toxicity profile further supports its potential for safe use in medical applications [40]. These results are consistent with the beneficial attributes observed in the present study of alginate.

The results regarding alginate's lack of significant enhancement in cisplatin's cytotoxicity, while less impactful compared to fucoidan, raise important points for further exploration. Alginate's primary role is often as a drug delivery matrix or protective agent rather than a direct enhancer of cytotoxicity. Studies have shown that alginate can reduce drug efficacy due to its ability to encapsulate and slow drug release, limiting immediate cytotoxic action [41]. In contrast, fucoidan's sulfated structure allows for better interaction with cellular components and may enhance chemotherapy effects by promoting apoptosis and oxidative stress [42].

Fucoidan exhibits notable anti-inflammatory activity, demonstrated through its ability to inhibit various inflammatory pathways. It reduces the production of key pro-inflammatory cytokines, such as TNF-α, IL-1β, and IL-6, *in vitro* and *in vivo*

models [43]. For instance, fucoidan from different algae species has shown efficacy in decreasing cytokine levels in stimulated human cells and macrophages. Specifically, low molecular weight fucoidan subfractions are particularly effective, as seen in the anti-inflammatory effects of LJSF4 from Saccharina japonica [44] and EMSF6 from Ecklonia maxima [45]. These fucoidans work by modulating signaling pathways like MAPK and NF-κB, highlighting their potential for therapeutic applications against inflammation. These results are consistent with the beneficial anti-inflammatory effects observed in the present study of fucoidan.

Alginate exhibits significant anti-inflammatory activity across various models. Alginate oligosaccharides reduce nitric oxide and pro-inflammatory cytokines such as TNF-α, IL-1β, and IL-6 in LPS-induced RAW 264.7 cells, showing peak anti-inflammatory effects after 36 hours of incubation. They also reduce NF-κB p65, iNOS, and COX-2 expression, decreasing ear edema and mast cell numbers [46]. Additionally, alginate microspheres enhance phagocytosis and modulate M1 macrophage responses, leading to a moderate reduction in bacterial viability and increased secretion of pro-inflammatory cytokines [47]. Sodium alginate, administered orally, significantly reduces inflammation and cytokine levels in a rat model of ulcerative colitis, demonstrating its therapeutic potential in managing chronic inflammatory conditions [48]. These findings highlight alginate's potential as an anti-inflammatory agent, which aligns with the findings of this study.

Seaweed bioactive compounds, such as fucoidan, exhibit diverse anticancer activities when tested alone or in combination with drugs like cisplatin. In 3D cultures, where cells often display greater resistance to treatments due to factors like hypoxia and altered drug diffusion, the effects of these compounds can differ significantly from those observed in 2D cultures. For instance, while fucoidan alone may have varying impacts on cytotoxicity, its combination with cisplatin can enhance or diminish drug effectiveness depending on the specific cell line and experimental conditions. This variability underscores the importance of 3D models for more accurate evaluations of drug interactions and therapeutic potentials [49]. 3D cell culture systems are becoming more precise drug testing models than traditional two-dimensional (2D) cultures. Studies have shown that 3D cultures, particularly those forming dense multicellular spheroids (MCSs), exhibit greater resistance to chemotherapeutic drugs like paclitaxel and doxorubicin due to factors such as hypoxia and altered apoptosis pathways. For example, breast cancer cell lines with dense MCSs in 3D cultures demonstrated reduced drug-induced apoptosis and changes in drug sensitivity compared to their 2D counterparts. This resistance is linked to higher proportions of dormant cells (G_0 phase) and lower levels of apoptotic markers [50]. Analysis of colon cancer spheroids showed lower activity in key signaling pathways like AKT, mTOR, and S6K in 3D models. Spatial variations in signaling were observed, with reduced phosphorylation of RPS6 at the spheroid core, mirroring *in vivo* tumor conditions. 3D cultures displayed enhanced antitumor responses to pathway inhibitors, such as increased ERK phosphorylation when AKT-mTOR-S6K was inhibited, contrary to 2D cultures. Additionally, MEK1 inhibition decreased AKT-mTOR-S6K signaling in 3D but not in 2D [51]. These findings highlight the distinct signaling rewiring in 3D models and their potential to mimic tumor behavior and improve anticancer drug evaluation.

This study has several limitations that warrant acknowledgment. First, the use of only one cell line (MDA-MB-231) limits the generalizability of the findings across different cancer subtypes. Second, the abnormal spectrogram data observed in the FTIR analysis of fucoidan points to potential impurities or instrumental limitations. While this analysis was conducted to confirm the presence of fucoidan, the spectroscopic

anomalies suggest that further refinement of the extraction process or improved purification methods may be needed.

5. Conclusion

This study highlights the potential of fucoidan extract of *S. ilicifolium* in overcoming cisplatin resistance, reducing drug dosage, and enhancing its effectiveness. The results demonstrate that fucoidan-rich extract exhibits dose-dependent antiproliferative effects and significantly improves the antitumor efficacy of cisplatin in both 2D and 3D models. Additionally, this extract shows notable anti-inflammatory and antioxidant properties, considerably reducing the secretion of cytokines IL-6 and IL-1β. Consequently, this study underscores the potential of fucoidan in addressing drug resistance, a significant challenge in cancer treatment, and may lead to more effective therapeutic strategies, thereby improving prognosis and quality of life for patients with drug-resistant breast cancer. The evidence suggests that combining fucoidan with cisplatin could enhance survival rates and reduce the social and economic burden of triple-negative breast cancer (TNBC), offering hope for more effective alternative treatments. Further investigation into these mechanistic differences between alginate and fucoidan and also can investigate the impact of these compounds on additional cancer cell lines.

Acknowledgements

The authors would like to express their gratitude to the research team members who contributed their time and expertise.

Conflict of interest

The authors declare no conflict of interest.

Author details

Reza Taghipour[1], Hadi Hassannia[2], Hesamoddin Arabnozari[3], Seyed Ehsan Enderami[4] and Emran Habibi[5]*

1 Faculty of Pharmacy, Mazandaran University of Medical Sciences, Sari, Iran

2 Immunogenetic Research Center, Faculty of Medicine and Amol Faculty of Paramedical Sciences, University of Medical Sciences, Sari, Iran

3 School of Medicine, Babol University of Medical Sciences, Babol, Iran

4 Immunogenetics Research Center, Department of Medical Biotechnology, School of Advanced Technologies in Medicine, Mazandaran University of Medical Sciences, Sari, Iran

5 Medicinal Plants Research Center, Mazandaran University of Medical Sciences, Sari, Iran

*Address all correspondence to: emrapharm@yahoo.com

IntechOpen

References

[1] Shokrzadeh M, Rajabali F, Habibi E, Modanloo M. Survey cytotoxicity and genotoxicity of hydroalcoholic extract of Stevia rebaudiana in breast cancer cell line (MCF7) and human fetallung fibroblasts (MRC-5). Journal of Cancer Research Metastasis. 2018;**1**(2):12-17

[2] Sanjeewa KA, Lee J-S, Kim W-S, Jeon Y-J. The potential of brown-algae polysaccharides for the development of anticancer agents: An update on anticancer effects reported for fucoidan and laminaran. Carbohydrate Polymers. 2017;**177**:451-459

[3] Smolarz B, Nowak AZ, Romanowicz H. Breast cancer—Epidemiology, classification, pathogenesis and treatment (review of literature). Cancers. 2022;**14**(10):2569

[4] Makki J. Diversity of breast carcinoma: Histological subtypes and clinical relevance. Clinical Medicine Insights: Pathology. 2015;**8**:23-31

[5] Derakhshan F, Reis-Filho JS. Pathogenesis of triple-negative breast cancer. Annual Review of Pathology: Mechanisms of Disease. 2022;**17**(1):181-204

[6] Howard FM, Olopade OI. Epidemiology of triple-negative breast cancer: A review. The Cancer Journal. 2021;**27**(1):8-16

[7] Liu S, Dong Y, Wang Y, Hu P, Wang J, Wang RY. Pristimerin exerts antitumor activity against MDA-MB-231 triple-negative breast cancer cells by reversing of epithelial-mesenchymal transition via downregulation of integrin β3. Biomedical Journal. 2021;**44**(6):S84-S92

[8] Van den Boogaard W, Komninos D, Vermeij W. Chemotherapy side-effects: Not all DNA damage is equal. Cancers. 2022;**14**(3):627

[9] Varghese E, Samuel SM, Líšková A, Samec M, Kubatka P, Büsselberg D. Targeting glucose metabolism to overcome resistance to anticancer chemotherapy in breast cancer. Cancers. 2020;**12**(8):2252

[10] Romani AM. Cisplatin in cancer treatment. Biochemical Pharmacology. 2022;**206**:115323

[11] Hill DP, Harper A, Malcolm J, McAndrews MS, Mockus SM, Patterson SE, et al. Cisplatin-resistant triple-negative breast cancer subtypes: Multiple mechanisms of resistance. BMC Cancer. 2019;**19**:1-13

[12] Sumithra M, Chitra V, Ramasamy R. Spectral analysis of Sargassum ilicifolium (turner) C. Agardh and *in vitro* anti-proliferative study of its ethanolic extract and chloroform fraction against colon cancer (HT-29) and lung cancer (A549) cell lines. Marmara. The Pharmaceutical Journal. 2017;**21**(2):269-277

[13] Tsou M-H, Lee C-C, Wu Z-Y, Lee Z-H, Lin H-M. Bioactivity of crude fucoidan extracted from *Sargassum ilicifolium* (turner) C. Agardh. Scientific Reports. 2022;**12**(1):15916

[14] Chandraraj S, Prakash B, Navanath K. Immunomodulatory activities of ethyl acetate extracts of two marine sponges *Gelliodes fibrosa* and *Tedania anhelans* and brown algae *Sargassum ilicifolium* with reference to phagocytosis. Research Journal of Pharmaceutical, Biological and Chemical Sciences. 2010;**1**:302-307

[15] Al-Muqbali MHS, Al-Alawi A, Waly MI, Rahman MS. Anticancer

properties of fucoidans extracted from brown seaweed (*Sargassum ilicifolium*) in a rat model of gastric cancer. Canadian Journal of Clinical Nutrition. 2019;**7**(2):43-61

[16] Simón L, Arazo-Rusindo M, Quest AF, Mariotti-Celis MS. Phlorotannins: Novel orally administrated bioactive compounds that induce mitochondrial dysfunction and oxidative stress in cancer. Antioxidants. 2023;**12**(9):1734

[17] Bouissil S, El Alaoui-Talibi Z, Pierre G, Michaud P, El Modafar C, Delattre C. Use of alginate extracted from Moroccan brown algae to stimulate natural defense in date palm roots. Molecules. 2020;**25**(3):720

[18] Li B, Wei X-J, Sun J-L, Xu S-Y. Structural investigation of a fucoidan containing a fucose-free core from the brown seaweed, Hizikia fusiforme. Carbohydrate Research. 2006;**341**(9):1135-1146

[19] Flórez-Fernández N, Balboa EM, Domínguez H. Extraction and purification of fucoidan from marine sources. Encyclopedia of Marine Biotechnology. 2020;**2**:1093-1125

[20] Xi X, Wei X, Wang Y, Chu Q, Xiao J. Determination of tea polysaccharides in *Camellia sinensis* by a modified phenol-sulfuric acid method. Archives of Biological Sciences. 2010;**62**(3):669-676

[21] Jouybari HB, Valadan R, Mirzaee F, Karizno FB, Habibi E. Immunomodulatory activity of polysaccharide from *Trametes gibbosa* (Pers.) Fr (Basidiomycota, fungi) mediated by TLR4 signaling pathway. Advanced Biomedical Research. 2023;**12**(1):127

[22] Dalal SR, Hussein MH, El-Naggar NE-A, Mostafa SI, Shaaban-Dessuuki SA. Characterization of alginate extracted from *Sargassum latifolium* and its use in *Chlorella vulgaris* growth promotion and riboflavin drug delivery. Scientific Reports. 2021;**11**(1):16741

[23] Amerifar M, Arabnozari H, Shokrzadeh M, Habibi E. Evaluation of antioxidant properties and cytotoxicity of brown algae (nizamuddinia zanardinii) in uterine (hela) and pancreatic cancer cell lines (paca-2). Human & Experimental Toxicology. 2024;**43**:09603271241227228

[24] Arabnozari H, Shaki F, Najjari A, Sharifianjazi F, Sarker SD, Habibi E, et al. The effect of *Polygonum hyrcanicum* Rech. f. Hydroalcoholic extract on oxidative stress and nephropathy in alloxan-induced diabetic mice. Scientific Reports. 2024;**14**(1):18117

[25] Habibi E, Hemmati P, Arabnozari H, Khalili HA, Sharifianjazi F, Enderami SE, et al. Phytochemical analysis and immune-modulatory potential of *Trichaptum biforme* polysaccharides: Implications for cancer. International Journal of Biological Macromolecules. 2024;**280**:135691

[26] Geraghty R, Capes-Davis A, Davis J, Downward J, Freshney R, Knezevic I, et al. Guidelines for the use of cell lines in biomedical research. British Journal of Cancer. 2014;**111**(6):1021-1046

[27] Park DC, Yeo SG, Shin EY, Mok SC, Kim DH. Clusterin confers paclitaxel resistance in cervical cancer. Gynecologic Oncology. 2006;**103**(3):996-1000

[28] El Hassouni B, Mantini G, Petri GL, Capula M, Boyd L, Weinstein HN, et al. To combine or not combine: Drug interactions and tools for their analysis. Reflections from the EORTC-PAMM course on preclinical and early-phase clinical pharmacology. Anticancer Research. 2019;**39**(7):3303-3309

[29] Cutone A, Frioni A, Berlutti F, Valenti P, Musci G, Bonaccorsi di Patti MC. Lactoferrin prevents LPS-induced decrease of the iron exporter ferroportin in human monocytes/macrophages. Biometals. 2014;**27**:807-813

[30] Siddiqui N, Asawa S, Birru B, Baadhe R, Rao S. PCL-based composite scaffold matrices for tissue engineering applications. Molecular Biotechnology. 2018;**60**:506-532

[31] Ata FK, Yalcin S. The cisplatin, 5-fluorouracil, irinotecan, and gemcitabine treatment in resistant 2D and 3D model triple negative breast cancer cell line: ABCG2 expression data. Anti-Cancer Agents in Medicinal Chemistry (Formerly Current Medicinal Chemistry-Anti-Cancer Agents). 2022;**22**(2):371-377

[32] Arnold M, Morgan E, Rumgay H, Mafra A, Singh D, Laversanne M, et al. Current and future burden of breast cancer: Global statistics for 2020 and 2040. The Breast. 2022;**66**:15-23

[33] He L, Wick N, Germans SK, Peng Y. The role of breast cancer stem cells in chemoresistance and metastasis in triple-negative breast cancer. Cancers. 2021;**13**(24):6209

[34] Al Monla R, Dassouki Z, Sari-Chmayssem N, Mawlawi H, Gali-Muhtasib H. Fucoidan and alginate from the brown algae *Colpomenia sinuosa* and their combination with vitamin C trigger apoptosis in colon cancer. Molecules. 2022;**27**(2):358

[35] Niknejad F, Kordjazi M, Asadi Farsani O, Sinehsepehr K. Cytotoxic effects of the fucoidan extracted from Persian gulf brown algae *Sargassum ilicifolium* inducing apoptosis in breast cancer cell line. Journal of Fisheries. 2022;**75**(1):63-73

[36] Xue M, Ge Y, Zhang J, Wang Q, Hou L, Liu Y, et al. Anticancer properties and mechanisms of fucoidan on mouse breast cancer *in vitro* and *in vivo*. PLoS One. 2012;**7**(8):e43483

[37] Gao W, Guo Y, Wang L, Jiang Y, Liu Z, Lin H. Ameliorative and protective effects of fucoidan and sodium alginate against lead-induced oxidative stress in Sprague Dawley rats. International Journal of Biological Macromolecules. 2020;**158**:662-669

[38] He X, Xue M, Jiang S, Li W, Yu J, Xiang S. Fucoidan promotes apoptosis and inhibits EMT of breast cancer cells. Biological and Pharmaceutical Bulletin. 2019;**42**(3):442-447

[39] Lachowicz D, Karabasz A, Bzowska M, Szuwarzyński M, Karewicz A, Nowakowska M. Blood-compatible, stable micelles of sodium alginate–curcumin bioconjugate for anti-cancer applications. European Polymer Journal. 2019;**113**:208-219

[40] Hoan NX, Anh LTH, Ha HT, Cuong DX. Antioxidant activities, anticancer activity, physico-chemistry characteristics, and acute toxicity of alginate/lignin polymer. Molecules. 2023;**28**(13):5181

[41] Sun J, Tan H. Alginate-based biomaterials for regenerative medicine applications. Materials. 2013;**6**(4):1285-1309

[42] Ale MT, Maruyama H, Tamauchi H, Mikkelsen JD, Meyer AS. Fucoidan from *Sargassum* sp. and Fucus vesiculosus reduces cell viability of lung carcinoma and melanoma cells *in vitro* and activates natural killer cells in mice *in vivo*. International Journal of Biological Macromolecules. 2011;**49**(3):331-336

[43] Ahmad T, Eapen MS, Ishaq M, Park AY, Karpiniec SS, Stringer DN,

et al. Anti-inflammatory activity of fucoidan extracts *in vitro*. Marine Drugs. 2021;**19**(12):702

[44] Ni L, Wang L, Fu X, Duan D, Jeon Y-J, Xu J, et al. *In vitro* and *in vivo* anti-inflammatory activities of a fucose-rich fucoidan isolated from *Saccharina japonica*. International Journal of Biological Macromolecules. 2020;**156**:717-729

[45] Lee H-G, Nagahawatta D, Liyanage N, Jayawardhana H, Yang F, Je J-G, et al. Structural characterization and anti-inflammatory activity of fucoidan isolated from *Ecklonia maxima* stipe. Algae. 2022;**37**(3):239-247

[46] Kim M-J, Bae N-Y, Bark S-W, Kim K-B-W-R, Park J-H, Park S-H, et al. Anti-inflammatory effect of alginate oligosaccharides produced by an alginate-degrading enzyme from *Shewanella oneidensis* PKA1008 on LPS-induced RAW 264.7 cells. Korean Journal of Fisheries and Aquatic Sciences. 2015;**48**(6):888-897

[47] Vaghasiya K, Eram A, Sharma A, Ray E, Adlakha S, Verma RK. Alginate microspheres elicit innate M1-inflammatory response in macrophages leading to bacillary killing. AAPS PharmSciTech. 2019;**20**:1-10

[48] Razavi A, Khodadadi A, Eslami MB, Eshraghi S, Mirshafiei A. Therapeutic effect of sodium alginate in experimental chronic ulcerative colitis. Iranian Journal of Allergy, Asthma, and Immunology. 2008;**7**(1):13-18

[49] Malhão F, Ramos AA, Macedo AC, Rocha E. Cytotoxicity of seaweed compounds, alone or combined to reference drugs, against breast cell lines cultured in 2D and 3D. Toxics. 2021;**9**(2):24

[50] Imamura Y, Mukohara T, Shimono Y, Funakoshi Y, Chayahara N, Toyoda M, et al. Comparison of 2D-and 3D-culture models as drug-testing platforms in breast cancer. Oncology Reports. 2015;**33**(4):1837-1843

[51] Riedl A, Schlederer M, Pudelko K, Stadler M, Walter S, Unterleuthner D, et al. Comparison of cancer cells in 2D vs 3D culture reveals differences in AKT–mTOR–S6K signaling and drug responses. Journal of Cell Science. 2017;**130**(1):203-218